Fractals, Vol. 9, No. 3 (2001) 287–295

PYRAMIDAL NEURONES IN MACAQUE VISUAL CORTEX: INTERAREAL PHENOTYPIC VARIATION OF DENDRITIC BRANCHING PATTERNS

HERBERT F. JELINEK* and GUY N. ELSTON†
*School of Community Health,
Faculty of Health Studies,
Charles Sturt University,
New South Wales, 2640, Australia
† Vision, Touch and Hearing Research Centre,
Department of Physiology and Pharmacology,
The University of Queensland, Qld, 4072, Australia
E-mail: G. Elston@vthrc.uq.edu.au

Received February 20, 2001; Accepted March 9, 2001

Abstract

The basal dendritic arbors of over 500-layer III pyramidal neurones of the macaque cortex were compared by fractal analyses, which provides a measure of the space filling (or branching pattern) of dendritic arbors. Fractal values (D) of individual cells were compared between the cytochrome oxidase (CO)-rich blobs and CO-poor interblobs of middle and upper layer III, and between sublaminae, in the primary visual area (V1). These data were compared with those in the CO compartments in the second visual area (V2), and seven other extrastriate cortical areas (V4, MT, LIP, 7a, TEO, TE and STP). There were significant differences in the fractal dimensions, and therefore the dendritic branching patterns, of cells in striate and extrastriate areas. Of the 55 possible pairwise comparisons of fractal dimension of neurones in different cortical areas (or CO compartments), 39 proved to be significantly different. The markedly different morphologies of pyramidal cells in the different cortical areas may be one of the features that determine the functional signatures of these cells by influencing the number of inputs received by, and propagation of potentials through, their dendritic arbors.

1. INTRODUCTION

The application of recently developed methodologies such as patch clamp recording and imaging has provided new insights into the importance of dendritic structure for cellular processing. The structure of dendritic arbors may influence the integration of inputs by individual cells in a number of different ways. For example, the number of bifurcations, length and diameter of the dendrites, and the distribution of inputs within the arbor, reportedly affect the propagation of potentials to the somata of neurones. Furthermore, the number of branches influences the spread of back propagating potentials within dendritic arbors (see Refs. 1–5 for reviews).

Recent studies have shown that pyramidal cells, the principal projection neurone of the cerebral cortex, show marked phenotypic variation amongst different cortical areas.[6–9] Differences in the number of branches, and spines, in the arbors of cells in diverse visual areas result in the potential to integrate different numbers of inputs, which may result in highly specialized processing (e.g. Ref. 9). Given that dendritic branching patterns are also critical in determining the potential for compartmentalization of processing within their arbors, it is essential that interareal differences in dendritic branching patterns be quantified if we are to better understand specialized aspects of cellular function in the cerebral cortex. Whilst previous studies have documented differences in various aspects of cell morphology in macaque visual cortex,[6,10,11] data were analyzed *a priori* according to the processing pathways of Ungerleider and Mishkin.[12] Aspects of pyramidal cell morphology have not yet been compared objectively across cortical areas. Moreover, branching patterns of the basal dendritic arbors of pyramidal cells have not been compared across processing pathways.

Fractal analyses allows the objective determination of the complexity, or space filling capacity, of dendritic arbors. Although it is controversial as to whether biological objects are fractal in nature,[13,14] the methodology provides a useful tool for making relative comparisons of the morphology of populations of cells.[15–18] Moreover, aspects of cell morphology, as revealed by fractal analyses, may be correlated with functional properties of different populations of cells.[19–24] In the present study, we used the dilation method to determine the fractal dimension (D) of individual layer III pyramidal neurones in nine different cortical areas involved in visual processing. We found that of 55 possible interareal comparisons of D values, 39 were significantly different (71%), revealing hitherto unknown variation in the branching patterns of pyramidal cells in the macaque cerebral cortex.

2. MATERIALS AND METHODS

2.1 Cell Injection, Immunohistochemistry and Cell Reconstruction

Cells for the present study were obtained from six macaque monkeys (*Macaca fascicularis*) between 14 to 28 months of age (Table 1). All cells were the same as used in previous studies.[6,10,11] Methods of cell injection, immunohistochemical processing, cell classification, and identification of visual areas have been outlined in previous studies.[10,25,26] Briefly, cells were injected with Lucifer Yellow (8% in 0.1 M Tris buffer, pH 7.4) by continuous current. Following injection of neurones, the sections were first processed with an antibody to Lucifer Yellow (1 : 400000 in stock solution [2% bovine serum albumin (Sigma A3425), 1% Triton X-100 (BDH 30632), 5% sucrose in 0.1 mol/l phosphate buffer]), then with a biotinylated species-specific secondary antibody (Amersham RPN 1004; 1 : 200 in stock solution), followed

Table 1 Animals from which data were collected.

Animal	Age (months)	Sex	Weight (kg)	Areas Studied
RM12	28	male	1.7	V1(IIIa/b)
RM13	20	male	1.5	V1(IIIc), 7a
AM1	14	male	1.3	V2, TEO
RM14	20	female	1.5	MT, LIP
SM1	23	male	1.5	V4
DM4	18	male	1.8	TE, STP

by a biotin-horseradish peroxidase complex (Amersham RPN1051; 1 : 200 in phosphate buffer). 3,3'-diaminobenzidine (Sigma D 8001) was used as the chromogen. Cells were analyzed by first drawing the complete basal dendritic arbor of each pyramidal neurone (in the plane parallel to the cortical surface) and digitizing the image using Adobe Photoshop and a VGA overlay frame grabber interface (Univision).

2.2 Fractal Analyses

Fractal analyses were performed using the public domain NIH Image Program (developed at the US National Institutes of Health, Bethesda, MD, and available on the Internet at *http://rsb.info.nih.gov/nih-image/*). Fractal analyses includes a number of different algorithms, such as box-counting, mass-radius and the dilation method. The dilation method based on the Minkowski-Bouligand dimension,[27–29] offers the advantage that it incorporates all points in the dendritic arbor, unlike the other methods, and is well suited for analyses of skeletonized images of dendrites.[23] The fractal dimension (D) was calculated for each cell by first replacing each pixel incorporated in the skeletonized image of the dendritic arbor with a 3×3 array of black pixels. The operation was then continued with successive passes, up to a maximum of 24, with successive pixel replacement over the cumulative image. Arrays that were smaller than the smallest part of the image, or larger than the width of the image, were excluded from the analysis, according to previously published criteria.[30] The length of the border for each respective diameter was then determined by dividing the area of the outline by the width of the array. D values were then estimated from the slope of the log-log plot of dendritic area vs. the width of the pixel array. The final D was calculated by subtracting the slope of the regression line from 2. If inclusion of all data points resulted in an r^2 of less than 0.995, those associated with the smallest array size were omitted from the plot until a better straight line fit ($r^2 \geq 0.996$) was obtained (see Ref. 30).

2.3 Statistical Analyses

Statistical analyses were made using the SPSS/PC+ software package (SPSS Inc., Chicago, IL.), and Statview for the Macintosh (Abacus Concepts Inc., Berkeley, CA). An analysis of variance was used to assess whether cell groups belonging to different cortical areas were significantly different. *Post-hoc* analyses included *t-tests* and Mann-Whitney U tests. If the data were normally distributed ($-0.5 < \text{skew} < 0.5$), *t-tests* were used, otherwise Mann-Whitney U tests were used.

3. RESULTS

3.1 Heterogeneity in the Fractal Dimension of Cortical Pyramidal Cells

Five hundred and eleven-layer III pyramidal cells from nine different cortical areas were included for analysis by the dilation method. Fractal values of cells were found to differ markedly between different cortical areas (Table 2), reflecting differences in their branching patterns (Fig. 1). Statistical analyses of D values revealed a significant difference in the data set, by cortical area ($F_{(510)} = 40.8$, $p < 0.01$). Of the 55 possible pairwise interareal comparisons of D values, 39 were found to be significantly different (71%: Table 3). Further analyses, assuming an *a priori* distinction between the dorsal and ventral visual processing pathways revealed systematic differences in the fractal dimensions of cells in the different cortical areas.

3.2 Variation of Fractal Dimensions Within Visual Pathways

Neurones in visual areas of the ventral stream differed such that there was a trend for an increase in fractal dimensions with progression through these cortical areas (i.e. V1<V2<V4<TEO<TE; Fig. 2). Comparison of the distribution of D values of neurones in the dorsal pathway revealed that those in middle and upper layer III of V1 had smaller D values than those in V2. Layer III pyramidal neurones in V2 had smaller D values than those in MT, as did layer IIIc pyramidal neurones in V1, which project directly to MT. Neurones in the lateral intraparietal area had larger D values than those in MT. However, neurones in area 7a had smaller D values than those in areas LIPv and MT (Fig. 2, Table 2). Neurones in the superior temporal polysensory area (STP), which reportedly occupies

Table 2 Fractal dimensions of cells in striate and extrastriate cortex.

Area	n	Mean	SD ($\times 10^{-1}$)	SEM ($\times 10^{-1}$)	Minimum	Maximum	Range
V1[a]	135	1.23	0.91	0.08	1.01	1.44	0.43
V1[b]	25	1.31	0.48	0.10	1.23	1.42	0.19
V2[c]	38	1.27	0.91	0.15	1.12	1.46	0.34
V2[d]	45	1.31	0.92	0.14	1.02	1.44	0.42
V4	34	1.29	0.82	0.14	1.09	1.44	0.35
TEO	44	1.39	0.67	0.10	1.12	1.57	0.45
TE	29	1.42	0.66	0.12	1.28	1.56	0.28
MT	34	1.40	0.46	0.08	1.30	1.50	0.20
LIP	39	1.42	0.53	0.09	1.26	1.55	0.29
7a	40	1.34	0.88	0.14	1.10	1.50	0.40
STP	29	1.44	0.45	0.08	1.34	1.51	0.17

[a]Data taken from middle and upper layer III.
[b]Data taken from layer IIIc.
[c]Data taken from the cytochrome oxidase-rich thin bands.
[d]Data taken from the cytochrome oxidase-rich thick bands.

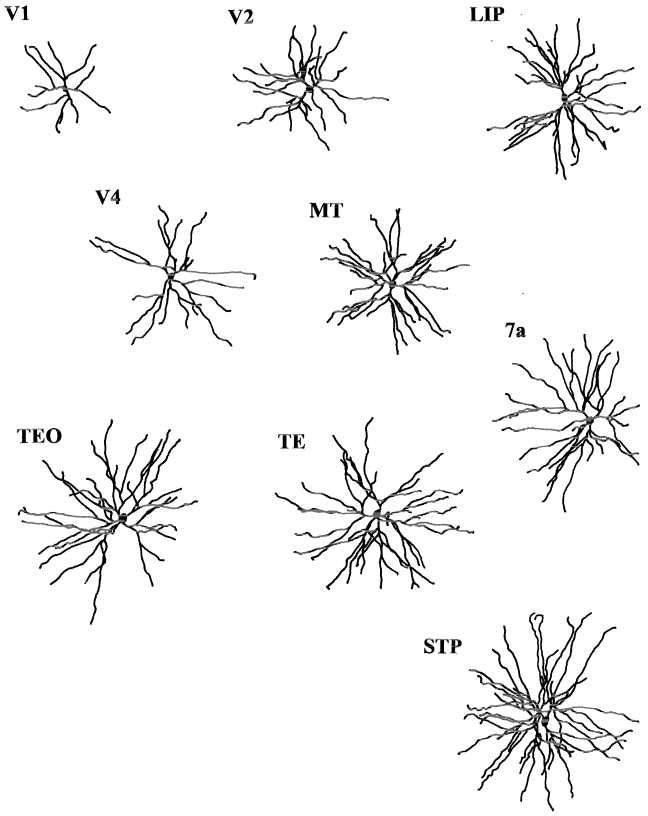

Fig. 1. Drawings of individual layer III pyramidal neurones in all cortical areas studied that had D values approximating the mean for each area. Cells are drawn in the tangential plane, revealing the arborization of the basal dendritic tree. The apical dendrite and colaterals are not illustrated, nor are the dendritic spines. In conjunction with the interareal differences in D values, the areas and spine densities of the basal dendritic fields also differ systematically between cortical areas (see Refs. 6, 10 and 11).

a higher level than all other cortical areas studied and contains cells which integrate across pathways,[31] had the greatest D values of all cells (Fig. 2).

3.3 Variation of Fractal Dimensions Across Visual Pathways

According to hierarchical models of visual processing (e.g. Ref. 32), cortical areas can be ranked at equivalent levels within the two pathways. For example, cortical areas MT and V4 reportedly occupy the third level, and areas 7a and TE reportedly occupy the fifth level, of the dorsal and ventral streams, respectively. The present results illustrate that the branching patterns of the dendritic arbors of pyramidal cells in these respective "pairs" of cortical areas clearly differ. Cells in area MT have, on average, a greater fractal dimension than those in area V4 (1.40 and 1.29, respectively), and cells in area TE have a greater fractal value than those in area 7a (1.42 and 1.34, respectively).

3.4 Modules in V1 and V2

Neurones in the different sublaminae of V1, which reportedly form the basis of projections to the two visual processing streams, had different distributions of their D values, reflecting the greater number of branches in the dendritic arbors of sublamina

Table 3 Statistical comparisons of D values of cells in different cortical areas.

	Ventral					Dorsal				
	V1	V2	V4	TEO	TE	V1	V2	MT	LIP	7a
V2	+									
V4	+	-								
TEO	+	+	+							
TE	+	+	+	-						
V1	+	-	-	+	+					
V2	+	+	-	+	+	-				
MT	+	+	+	-	-	+	+			
LIP	+	+	+	-	-	+	+	-		
7a	+	+	+	+	+	-	-	+	+	
STP	+	+	+	+	-	+	+	-	-	+

Note: Cortical areas are grouped according to the study of Felleman and van Essen.[32] Neurones in V1 and V2 are included in both pathways: data from layer IIIc of V1 and the cytochrome oxidase-rich thick bands of V2 are included in the dorsal stream, while those of middle and upper layer III in V1 and the cytochrome oxidase-rich thin bands in V2 are included in the ventral stream ($+p < 0.05$; $p \geq 0.05$).

IIIc as compared to those in sublaminae IIIa/b[10,11] (Fig. 2). A *post-hoc* t-test revealed the difference to be significant ($t_{(158)} = -4.24$, $p < 0.05$). However, there was no significant difference in the fractal dimensions of neurones in the blobs and interblobs in sublaminae IIIa/b of V1 ($U' = 1871$, $Z = -4.92$, $p = 0.622$). In V2, neurones in the cytochrome oxidase (CO)-rich thick bands had higher D values than those in the CO-rich thin and CO-poor interbands (Table 2), which proved to be significantly different (Table 3).

4. DISCUSSION

By using fractal analyses, we have demonstrated significant and systematic differences in the branching patterns of the basal dendritic change fields to trees of supragranular pyramidal neurones in different cortical areas of the macaque monkey. Objective analyses of the basal dendritic arbors of over 500 cells in the different cortical areas revealed that over 70% of possible pairwise interareal comparisons of fractal values were significantly different. These results support and extend previous findings of morphological heterogeneity of a specific cell type (pyramidal cell), within the same cortical layer, in cortical areas involved in visual processing.

4.1 Fractal Values in Cortical Visual Processing Pathways

There is a general trend for cells with larger, more complex and more spinous basal dendritic arbors in higher cortical areas in the proposed anatomical hierarchies.[6,10,11,33] The present data parallel those findings in the sense that, in general, cells in progressively "higher" cortical areas were characterized by progressively greater fractal dimensions (Fig. 2, Table 2). This trend was particularly striking in the ventral processing pathway, where there was a successive increase in fractal dimension of cells in cortical areas V1, V2, V4, TEO and TE. With one exception (area 7a), the fractal dimensions of cells in cortical areas of the dorsal pathways (V1, V2, MT and LIP) accord with the proposed cortical hierarchies of Felleman and van Essen.[32] Neurones in area STP, which reportedly integrate inputs from both the dorsal and ventral processing pathways and integrate polysensory inputs,[34,35] had higher fractal dimensions than those in all other areas studied in the occipital, parietal and temporal lobes.

4.2 Module-Specific Branching Patterns

As well as using fractal analyses to distinguish pyramidal cells in different cortical areas, we were able to distinguish subpopulations of cells reportedly associated with the two processing streams within the primary and second visual areas (see Refs. 10 and 11 for details). In V1, for example, neurones were analyzed according to which sublaminae they were located. Neurones in the different

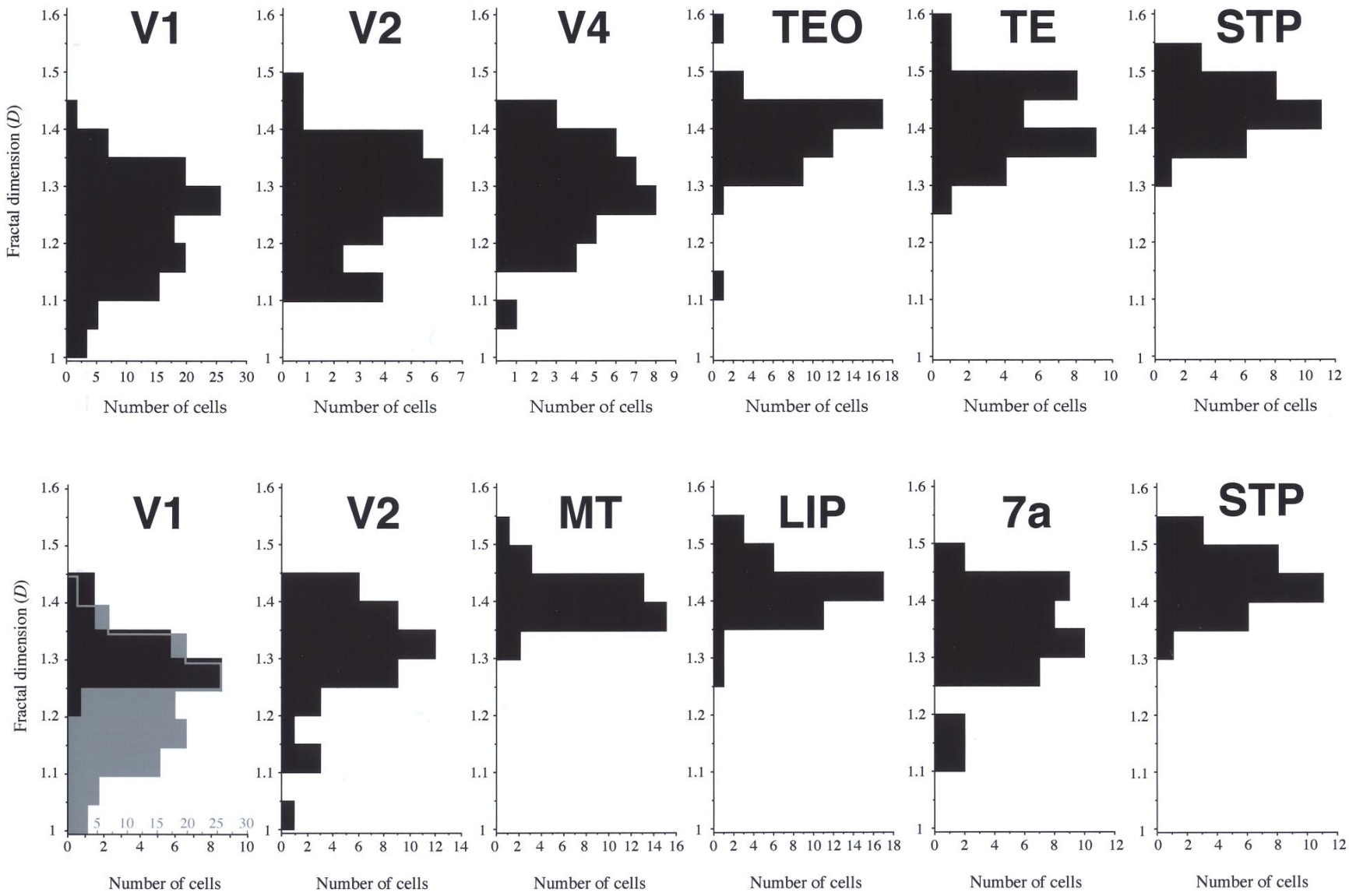

Fig. 2. Frequency histograms of D values of layer III pyramidal cells in visual cortical areas of the macaque monkey. Areas are arranged according to the processing pathways of Felleman and van Essen[32] and Gross et al.[31] Ventral stream data for V1 were sampled from middle and upper layer III, those of V2 included cells located at the base of layer III within the cytochrome oxidase (CO) thin bands. Dorsal stream data for V1 were sampled from sublamina IIIc, those of V2 were located at the base of layer III in the CO thick bands. Data for STP is illustrated in both pathways as it has been placed at the top of these pathways by various authors (e.g. Refs. 31 and 74).

sublaminae of V1 are reportedly incorporated in the different pathways: those in sublamina IIIc being part of the dorsal pathway whereas those in sublaminae IIIa/b are included in the ventral pathway[36–38] (but see Refs. 39–41). The present results show significant differences in the D values of pyramidal neurones in these different sublamina. However, while cells in the CO blobs are significantly larger than those in the interblobs and have different degrees of bias in their dendritic arbors,[11] we failed to find a significant difference in the D values of cells in these different CO compartments. Thus, some aspects of the dendritic and axonal arborizations of pyramidal neurones in these CO compartments differ significantly,[11,42] whereas other aspects of their morphology appear not to.

Similarly, neurones in V2 have been grouped into one of the two streams revealed by patterns of CO histochemistry. Briefly, neurones in the CO-rich thick bands reportedly receive projections from sublamina IIIc of V1, and project to area MT. Neurones in the CO-rich thin and interbands receive projections from middle and upper layer III and layer II of V1, and project to the ventral pathway.[43–46] We found a significant difference in the D values of layer III pyramidal neurones in these CO compartments in V2, whereas analyses of previously published data[10,11] revealed no significant difference in the size of the basal dendritic fields of neurones in the different CO compartments in V2. Thus, the results in both V1 and V2 highlight the importance of analyzing morphological features by a number of converging methodologies. Moreover, the overall results show that fractal analyses is a useful tool in distinguishing populations of functionally related, but different, pyramidal cells in cerebral cortex.

4.3 Methodological Considerations

Arguably, differences in the branching patterns of supragranular pyramidal cells in the different cortical areas may be attributed to inter-individual differences, area-specific rates of maturation or environmental factors.[47–50] However, comparison of cells in multiple areas, sampled from the same hemisphere, reveals consistent marked, and systematic, differences in cell structure.[33] Moreover, interareal comparisons of pyramidal cells in man,[51] macaque,[6,10,11] and marmoset[33] show similar trends for differences in the pyramidal cell phenotype in different cortical areas, despite the fact that data from each species represent different developmental ages.

Another possibility is that interareal differences in cell morphology presented here reflect differences in subpopulations of pyramidal cells which form projections to different regions. For example, morphology of pyramidal neurones within a given cortical layer may vary significantly according to their projection targets,[52–56] and the proportion of these cells may differ amongst cortical areas.[57–59] However, as cells in the present study were injected pseudo-randomly, any such difference would still reflect differences in circuitry in different cortical areas. Given the consistency of the trends for variation in the morphology of over 1500 pyramidal cells in different cortical areas in man, macaque and marmoset, we are reasonably confident that the results presented here reflect an organizational principal of the cerebral cortex of higher primates.

4.4 Functional Interpretations

As demonstrated originally by Rall,[60] nonlinear integration may lead to compartmentalization of processing within dendritic arbors (see Refs. 3, 5, 61–63 for reviews). The function significance of differing capabilities to compartmentalize inputs within pyramidal cell dendritic arbors was recently demonstrated by Poirazi and Mel[64] who showed that compartmentalization acts as a mechanism for boosting cellular potential for learning paradigms: a linear increase in the number of dendritic branches results in a logarithmic increase in input-output functions. Thus, pyramidal cells in areas such as TE and STP, which are characterized by large complex dendritic arbors (Ref. 6 and present results), may have greater functional capacity than smaller, less complex cells such as those in areas V1 and V2.

As well as affecting the retrograde propagation of potentials, orthograde, or "back" propagation[65–67] is also influenced by the structure of dendritic arbors (see Refs. 1, 4 and 68 for reviews). Decay of the back propagating potential, which serves to potentiate synchronously active inputs[69,70] throughout the dendritic arbor is crucially dependent on the number of branch points.[71] These features have not yet been tested rigorously in cortical pyramidal cells with markedly different *interareal* phenotypic variation, however, supragranular pyramidal cells in cortical areas V1 and TE show diametrically opposed responses following tetonic stimulation (i.e. LTP vs. LTD).[72] Furthermore, large spinous

cells characterized by complex branching patterns, such as those in temporal cortex, are capable of performing shape-dependent direction selectivity,[73] which may depend on compartmentalization of processing within their dendritic arbors. Further experiments are required to establish whether these functional differences may be partly attributable to differences in the propagation of potentials through dendritic arbors. Matching the differing morphologies of pyramidal cells in different cortical areas directly to functional characteristics remain exciting challenges for future studies.

LIST OF ABBREVIATIONS

D	Fractal dimension
LIP	Lateral intraparietal area
LTD	Long term depression
LTP	Long term potentiation
MT	Middle temporal area
STP	Superior temporal polysensory area
TE	Cytoarchitectonic area
TEO	Cytoarchitectonic area
V1	Primary visual area
V2	Second visual area
V4	Fourth visual area
7a	Subdivision of cytoarchitectonic area 7

ACKNOWLEDGEMENTS

We would like to thank Dr. David Vaney for generously allowing access to his intracellular injection laboratory and Dr. David Pow for providing his antibody to Lucifer Yellow. Tissue was kindly provided by Prof. Jack Pettigrew, and Dr's Marcello Rosa and Souyma Ghosh. We would also like to thank Dr. Marcello Rosa for comments on a previous version of the manuscript and Cherryl Kolbe and Blanca Hernández Charro for technical assistance. Supported by a CSU Faculty Seed Grant (HJ) and a CJ Martin Fellowship (GNE) and grant (990007) from the National Health and Medical Research Council of Australia.

REFERENCES

1. N. Spruston, G. Stuart and M. Häusser, in *Dendrites*, eds. G. Stuart, N. Spruston and M. Häusser (Oxford, New York, 1999), pp. 1–34.
2. I. Segev and M. London, in *Dendrites*, eds. G. Stuart, N. Spruston and M. Häusser (Oxford University Press, New York, 1999), pp. 205–230.
3. B. Mel, in *Dendrites*, eds. G. Stuart, N. Spruston and M. Häusser (Oxford University Press, New York, 1999), pp. 271–289.
4. M. Häusser, N. Spruston and G. J. Stuart, *Science* **290**, 739–744 (2000).
5. C. Koch. *Biophysics of Computation. Information Processing in Single Neurons* (Oxford University Press, New York, 1999).
6. G. N. Elston, R. Tweedale and M. G. P. Rosa, *Proc. R. Soc. Lond. Ser.* **B266**, 1367–1374 (1999).
7. G. N. Elston and M. G. P. Rosa, *J. Neurosci.* **20RC117**, 1–5 (2000).
8. J. S. Lund, T. Yoshioka and J. B. Levitt, *Cereb. Cortex* **3**, 148–162 (1993).
9. G. N. Elston, *J. Neurosci.* **20RC95**, 1–4 (2000).
10. G. N. Elston and M. G. P. Rosa, *Cereb. Cortex* **7**, 432–452 (1997).
11. G. N. Elston and M. G. P. Rosa, *Cereb. Cortex* **8**, 278–294 (1998).
12. L. G. Ungerleider and M. Mishkin, in *Analysis of Visual Behavior*, eds. D. J. Ingle, M. A. Goodale and R. J. W. Mansfield (MIT, Cambridge, 1982), pp. 549–586.
13. J. D. Murray, *J. Comp. Neurol.* **361**, 369–371 (1995).
14. J. Panico and P. Sterling, *J. Comp. Neurol.* **361**, 479–490 (1995).
15. F. Caserta, W. D. Eldred, E. Fernandez, R. E. Hausman, L. R. Stanford, S. V. Bulderev, S. Schwarzer and H. E. Stanley, *J. Neurosci. Meth.* **56**, 133–144 (1995).
16. L. L. Porter, S. Ghosh, G. D. Lange and T. G. Smith, *Neurosci. Lett.* **130**, 112–116 (1991).
17. A. Schierwagen, in *Organizational Constraints on the Dynamics of Evolution*, eds. J. Maynard-Smith and G. Vida (Manchester University Press, Manchester, 1990), pp. 167–189.
18. K. D. Kniffiki, M. Pawlak and C. Vahle-Heinz, *Fractals* **1**, 171–178 (1993).
19. A. Schierwagen, in *Chaos in Biological Systems*, eds. D. H. Holden and L. F. Olsen (Springer, Berlin, 1987), pp. 191–216.
20. E. A. Neale, L. M. Bowers and T. G. Smith, *J. Neurosci. Res.* **34**, 54–66 (1993).
21. T. G. Smith, K. Brauer and A. Reichenbach, *J. Comp. Neurol.* **331**, 402–406 (1993).
22. H. F. Jelinek and I. Spence, *Fractals* **5**, 673–684 (1997).
23. H. F. Jelinek and E. Fernandez, *J. Neurosci. Meth.* **81**, 9–18 (1998).
24. R. C. Cannon, H. V. Wheal and D. A. Turner, *J. Comp. Neurol.* **413**, 619–633 (1999).
25. G. Einstein, *J. Neurosci. Meth.* **26**, 95–103 (1988).
26. E. H. Buhl and W. Schlote, *Acta. Neuropathol.* **75**, 140–146 (1987).

27. M. Schroeder, *Fractals, Chaos and Power Laws* (Freeman and Co., New York, 1991).
28. B. B. Mandelbrot, *The Fractal Geometry of Nature* (Freeman and Co., New York, 1983).
29. A. G. Flook, *Powder Techn.* **21**, 295–298 (1978).
30. E. Fernandez and H. F. Jelinek, *Meths. Enzymol.*, in press (2001).
31. C. G. Gross, H. R. Rodman, P. M. Gochin and M. W. Colombo, in *Computational Learning and Recognition*: *Proceedings of the 3rd NEC Research Symposium*, ed. E. Baum (Society for Industrial and Applied Mathematics, Philadelphia, 1993), pp. 44–73.
32. D. J. Felleman and D. C. van Essen, *Cereb. Cortex* **1**, 1–47 (1991).
33. G. N. Elston, R. Tweedale and M. G. P. Rosa, *J. Comp. Neurol.* **415**, 33–51 (1999).
34. K. Hikosaka, E. Iwai, H. Saito and K. Tanaka, *J. Neurophysiol.* **60**, 1615–1637 (1988).
35. M. W. Oram and D. I. Perrett, *J. Neurophysiol.* **76**, 109–129 (1996).
36. M. S. Livingstone and D. H. Hubel, *J. Neurosci.* **7**, 3416–3468 (1987).
37. S. Shipp and S. Zeki, *Eur. J. Neurosci.* **1**, 333–354 (1989).
38. T. Yoshioka and B. M. Dow, *Behav. Brain Res.* **76**, 71–88 (1996).
39. A. Sawatari and E. M. Callaway, *Nature* **380**, 442–446 (1996).
40. J. S. Lund, Q. Wu, P. T. Hadingham and J. B. Levitt, *J. Anat.* **187**, 563–581 (1995).
41. J. S. Lund, T. Yoshioka and J. B. Levitt, "Primary Visual Cortex Primates," in *Cerebral Cortex*, eds. A. Peters and K. S. Rockland (Plenum, New York, 1994), Vol. 10, pp. 37–60.
42. N. H. Yabuta and E. M. Callaway, *Vis. Neurosci.* **15**, 1007–1027 (1998).
43. S. Shipp and S. Zeki, *Nature* **315**, 322–325 (1985).
44. H. Nakamura, R. Gatass, R. Desimone and L. Ungerleider, *J. Neurosci.* **13**, 3681–3691 (1993).
45. A. Roe and D. Y. T'so, *J. Neurosci.* **15**, 3689–3715 (1995).
46. D. J. Felleman, Y. Xiao and E. McClendon, *J. Neurosci.* **17**, 3185–3200 (1997).
47. B. Jacobs, L. Larsen-Driscoll and M. Schall, *J. Comp. Neurol.* **386**, 661–680 (1997).
48. B. Anderson and V. Rutledge, *Brain* **119**, 1983–1990 (1996).
49. S. Nakamura, I. Akiguchi, M. Kameyama and N. Mizuno, *Acta Neuropathol.* **65**, 281–284 (1985).
50. W. Greenough, F. R. Volkmar and J. M. Juraska, *Exp. Neurol.* **41**, 371–378 (1973).
51. G. N. Elston, R. Benavides-Piccione and J. DeFelipe, *J. Neurosci.*, in press (2001).
52. M. Hübener and J. Bolz, *Neurosci. Lett.* **94**, 76–81 (1988).
53. M. Hübener, C. Schwarz and J. Bolz, *J. Comp. Neurol.* **301**, 655–674 (1990).
54. B. G. Klein, R. D. Mooney, S. E. Fish and R. W. Rhodes, *Neuroscience* **17**, 57–78 (1986).
55. J. A. Matsubara, R. Chase and M. Thejomayen, *J. Comp. Neurol.* **366**, 93–108 (1996).
56. D. M. Vogt Weisenhorn, R.-B. Illing and W. B. Spatz, *J. Comp. Neurol.* **362**, 233–255 (1995).
57. D. C. van Essen, W. T. Newsome and J. L. Bixby, *J. Neurosci.* **2**, 265–283 (1982).
58. M. G. P. Rosa, "Visuotopic Organization of Primate Extrastriate Cortex," in *Cerebral Cortex*, eds. K. Rockland, J. H. Kaas and A. Peters (Plenum, New York, 1997), Vol. 12, pp. 127–204.
59. K. S. Rockland, "Elements of Cortical Architecture: Hierarchy Revisited," in *Cerebral Cortex*, eds. K. Rockland, J. H. Kaas and A. Peters (Plenum, New York, 1997), Vol. 12, 243–293.
60. W. Rall, in *Neural Theory and Modeling*, ed. R. F. Reiss (Stanford University Press, Stanford, 1964), pp. 73–97.
61. W. Rall, R. E. Burke, W. R. Holmes, J. J. B. Jack, S. R. Redman and I. Segev, *Physiol. Rev.* **72**, 159–186 (1992).
62. I. Segev, *Nature* **393**, 207–208 (1998).
63. Z. F. Mainen and T. J. Sejnowski, *Nature* **382**, 363–366 (1996).
64. P. Poirazi and B. Mel, *Neuron* **29**, 779–796 (2001).
65. G. J. Stuart and B. Sackman, *Nature* **367**, 69–72 (1994).
66. G. J. Stuart and M. Häusser, *Neuron* **13**, 703–712 (1994).
67. N. Spruston, Y. Schiller, G. Stuart and B. Sackman, *Science* **268**, 297–300 (1995).
68. G. J. Stuart, N. Spruston, B. Sackman and M. Häusser, *Trends Neurosci.* **20**, 125–131 (1997).
69. J. C. Magee and D. Johnston, *Science* **275**, 209–213 (1997).
70. H. Markram, J. Lübke, M. Frotscher and B. Sackman, *Science* **275**, 213–215 (1997).
71. P. Vetter, A. Roth and M. Häusser, *J. Neurophysiol.* **85**, 926–937 (2001).
72. Y. Murayama, I. Fujita and M. Kato, *Neuroreport* **8**, 1503–1508 (1997).
73. K. Tanaka, T. Koyama and A. Mikami, *Neuroreport* **10**, 393–397 (1999).
74. M. S. A. Graziano and C. G. Gross, in *The Association Cortex*, *Structure and Function*, eds. H. Sakata, A. Mikami and J. Fuster (Harwood Academic Publishers, Amsterdam, 1997), pp. 219–232.